STUDIES ON A RHOMBIC ANTENNA WITH CYLINDRICAL HELICES AS THE ARMS

ASHOKE KUMAR SEN

Institute of Radio Physics and Electronics, University of Calcutta

(*Received for publication, April* 2, 1958)

ABSTRACT. The input impedance and the directivity of a rhombic antenna with arms in the form of cylindrical helices of constant pitch angle have been studied.

On the basis of certain plausible assumptions, theoretical expressions have been derived to obtain the input impedance and the directivity of the antenna. The results have been compared with experimentally observed values.

1. INTRODUCTION

The rhombic antenna is widely used in military and commercial services for point-to-point communication. It is a wide band antenna and possesses substantial degree of directivity. These two properties, as is well-known, result from the aperiodic nature of the system. The rhombic antenna, however, suffers from a number of limitations mentioned below:

(i) The horizontal and vertical radiation patterns being perceptibly dependent on one another, it is impossible to obtain high angle radiation except at very low gain and for very broad horizontal pattern;

(ii) Wastage of input energy at the terminating resistor, thereby greatly reducing the efficiency of the system;

(iii) Large plot of land is necessary for its erection.

The first difficulty is reduced to a considerable extent by using arrays of rhombic antennas in cascade, which, in addition, suppress smaller unwanted lobes of radiation and improve the radiation efficiency. The second difficulty is effectively minimised if the input impedance of the antenna is lowered by using multiple wires (space-tapered) instead of single conductors constituting the arms and also by feeding the energy at the terminal end back to the system in a manner that progressive waves flow round the network (Neimann, 1939).

In an attempt to reduce the third difficulty, the present author has investigated the possibility using cylindrical helices as the arms of the rhombic antenna. In a helix, the "axial" velocity of the electric wave is less than that along a linear conductor so that a rhombic antenna with helices as the arms should in effect correspond to a much longer rhombic antenna with linear arms. The antenna studied consists in each arm a helix designed for a midfrequency of

600 mc/s. The pitch angle and the length of each turn are 12° and 20 cm. respectively so that the helix operates predominantly in the "normal" mode over the entire frequency band.

The impedance characteristics and the radiation pattern of this antenna have been studied both theoretically and experimentally. The results of these investigations are reported in this paper.

2. EXPERIMENTAL ARRANGEMENTS AND MEASUREMENTS

The rhombic antenna has been designed to operate in the frequency range of 300 mc/s to 900 mc/s with the mid-frequency of 600 mc/s. Each arm of the antenna consists of a cylindrical helix of 10 turns made of hard-drawn copper-wire (1/8″ in diameter). The pitch angle of the helix is about 12° and the length of the wire in each turn is 20 cm. The total length of wire in each helix is 200 cm; that is, 4 wavelengths at the mid-frequency. The axial length of the helix is 40 cm. The inclination between the arms is made according to the standard design chart for the ordinary rhombic antenna (Smith, 1948), its value being about 145°. The included angle is adjusted to 35° so that the first maximum lobe may be directed along the major axis of the rhombus and its elevation is of the order of 17.5°. The elevation 17.5° is chosen because of convenience in the measurement of radiation patterns. The antenna is mounted horizontally over a copper-wire net at a height of about 3.75 wavelengths (corresponding to 600 mc/s) which satisfies the condition of maximum field intensity at the elevation angle of 17.5°. The copper net of close mesh provides the perfect "ground".

(i) *Measurement of impedance* :

The layout of the rhombic antenna with its measuring devices is shown in figure 1. The input impedance is measured by means of a twin-wire standing-

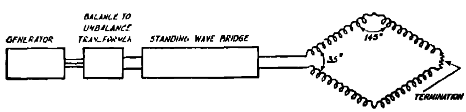

Fig. 1.—Block diagram of the experimental arrangement for the measurement of input impedance of the antenna.

wave bridge designed and constructed for the experiment. A balance-to-unbalance transformer is incorporated at the input end of the bridge since the generator output is taken through a co-axial cable.

Several wavelengths of line are placed between the bridge and the antenna, thereby eliminating the need for locating symmetrically both the operator and the measuring equipment. The line length, however, is so chosen that the attenuation introduced by it may be neglected (Tomiyasu, 1949). The measurements have been made at frequencies from 300 mc/s to 900 mc/s. The impedance-frequency and standing-wave ratio characteristics are shown in figures 2-3.

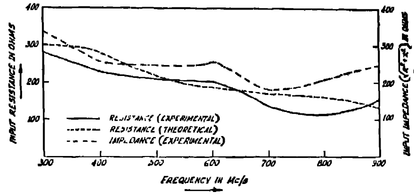

Fig 2.—Illustrating the variation of the calculated (dotted line) and the observed (solid line) values of the input resistance with frequency. Observed (chain line) values of input impedance $\sqrt{R^2+X^2}$ is also shown. Frequency range: 300 Mc/s to 900 Mc/s..

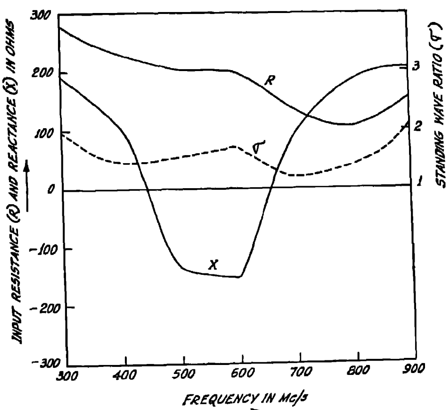

Fig. 3.—Observed values of the resistive (R) and the reactive (X) parts of the input impedance and also the SWR characteristics. Frequency range: 300 Mc/s to 900 Mc/s.

(ii) *Measurement of radiation pattern* :

The antenna together with the balance-to-unbalance transformer and the tapered feeder for impedance matching are erected horizontally above the ground. The height of the antenna from the copper net of close mesh which acts as ground, is adjusted so that the major radiation lobe satisfies the condition of maximum field intensity for an ordinary rhombic antenna. The receiving antenna is a dipole placed at a distance of about 10 wavelengths (corresponding to 600 mc/s) from the antenna under study. The height of the dipole is adjusted so that it receives maximum "illumination" from the major radiation lobe, which makes an angle of 17.5° approximately with the plane of the rhombic antenna.

Imperfect termination of the antenna over the frequency-band generates back radiation due to the standing waves on the conductor arms, but its magnitude has been found to be small. Consequently, the measurement of the radiation pattern has been made only in the forward direction and the test antenna is swept through an angle of 180°. Both horizontally and vertically polarised components of the field have been measured only in the horizontal plane. The vertical-plane patterns, however, could not be measured because of experimental difficulties.

The crystal detector being a square-law device, accurate measurement of small side-lobe amplitudes is difficult. Hence, only the major lobes at different frequencies have been measured. The tendency of the major lobe to split up at the higher end of the frequency band has been shown in one particular case (figure 7f).

The plots of radiation patterns for different frequencies are shown in the figures 7–9.

3. THEORETICAL CONSIDERATIONS

(i) *Calculation of impedance* :

An approximate formula for the average characteristic impedance of the antenna has been derived by the standard method based on Schelkunoff's treatment of the biconical antenna (Schelkunoff, 1943). For the biconical antenna, Schelkunoff assumes that only the TEM transmission mode is present, so that both E and H lines are entirely transverse, that is, they have no radial component. This satisfies the boundary conditions since E is normal to the surface of the cones and the H lines are circles lying in planes normal to the polar axis. The voltage between points 1 and 2 on the cones at a distance r (figure 4) from the terminals is given by

$$V(r) = \int_{\theta_{hc}}^{\pi-\theta_{hc}} E_\theta \, . \, r d\theta \qquad \ldots \quad (1)$$

where θ_{hc} is the half-angle of the cone.

The total current $I_{(r)}$ at the same point is obtained by Ampere's law,

$$I_{(r)} = \int_0^{2\pi} H\phi r \sin\theta d\phi = 2\pi r \sin\theta H\phi \qquad \ldots \quad (2)$$

If the biconical antenna is considered infinitely long, the ratio of $V_{(r)}$ and $I_{(r)}$ given by Eqns. (1) and (2) would give the characteristic impedance of the antenna

In the case of a rhombic antenna with cylindrical helices as the arms, the situation is evidently more complicated. For the sake of simplification, however, certain plausible assumptions may be made. These are discussed below:

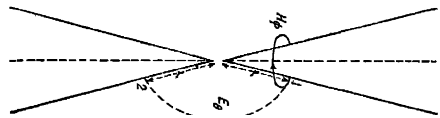

Fig. 4.—E_θ and H_φ lines of outgoing TEM wave on a biconical antenna.

(a) The average characteristic impedance of a rhombic antenna is approximately equal to the input impedance of infinitely long diverging wires of the same included angle (Scholkunoff, 1952).

(b) When two conical conductors of equal cone angles are kept inclined to each other symmetrically with repsect to a centre axis and are fed at the apex, the system radiates. Schelkunoff and others have shown that the interaction between the two diverging conductors may be neglected except in the vicinity of the input ends when the gap at the input end is large compared to the average radius of the conductors. On similar grounds we have also neglected any possible effect due to interaction between the arms of the antenna under study. Hence, the electromagnetic field may be considered uniform in the intervening region between the arms.

(c) It is known that strictly transverse electromagnetic waves cannot exist on non-conical wires (Schelkunoff, 1952). In the case of a helix, the field contains a voltage component due to the circumferential magnetic flux. But its magnitude being in our case relatively small, it may be neglected. The electromagnetic waves in the intervening region between the two arms may thus be assumed to be entirely transverse, as done by Schelkunoff in his treatment of the biconical antenna. The electric lines of force between the two arms, hence, will run principally along the great circles passing through the axes of the helix arms and the voltage will be the line integral of this electric field along the great circle.

(d) Since the antenna is terminated by its characteristic impedance and the conductors are assumed to be loss-less, the current distribution along the arms may be assumed uniform. Standing waves are, however, likely to exist on the conductors due to irregularities introduced at the side corners of the rhombic antenna and also due to the variation of characteristic impedance from point to point along the two diverging conductors. But these effects are usually negligible (Schelkunoff, 1952) and so, the current in the arm is primarily progressive. Consequently the principal wavefronts are spherical in nature. The effect is, therefore, like that of a current flowing 'axially' along the helices, the velocity of which is a function of the helix parameters. Pocklington (1897) has shown that for a helix of dimensions comparable to the wavelength, the axial velocity is given by

$$v = c \sin \alpha \qquad \dots \quad (3)$$

where v is the phase velocity of the axial current; c, the velocity of light (3×10^{10} cm/sec.); and α, the pitch angle of the helix.

Since the field in the intervening region between the two arms is assumed entirely transverse, both E and H components can be expressed in terms of scalar potential functions. The potential function for the progressive travelling waves may be written as

$$T = A[K_0(\beta_{r1})-K_0(\beta_{r2})] \qquad \dots \quad (4)$$

where A is a constant; β, the axial phase constant $\left(=\frac{\omega}{v}\right)$; ω, the frequency in radians/sec., r_1 and r_2, the distances from the axes of the helix-arms of a point P in space on the meridian plane (figure 5), and K_0 is the modified Bessel function which is the solution of the modified Bessel equation of order zero, with the independent variable β_r. It is known that the modified Bessel equation has two independent solutions involving I_0 and K_0. I_0, which is finite for all values of r and is only appropriate for source-free regions, is disregarded. The K_0-function however, vanishes at infinity and is retained, since it represents an outward travelling wave.

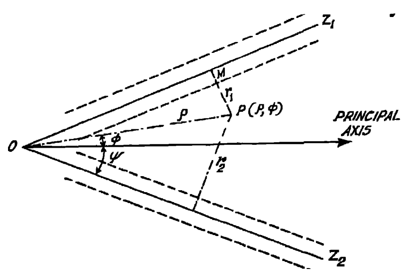

Fig. 5.—Illustrating the calculation of distance of a point 'P' in space from the two inclined arms of the antenna. The dotted lines indicate the outlines of the cylindrical helices and the solid lines OZ_1 and OZ_2, the axes thereof.

In figure 5, 2ψ is the included angle between the arms and (ρ, ϕ) are the co-ordinates of the reference point P on the meridian plane. Expressing r_1 and r_2 in terms of ρ, ψ and ϕ, the potential function takes the form

$$T = A[K_0\{\beta\rho \sin(\psi-\phi)\}-K_0\{\beta\rho \sin(\psi+\phi)\}] \qquad \dots \quad (5)$$

The azimuthal component of the magnetic field at P is given by the relation,

$$H\phi = -\frac{1}{\rho}\cdot\frac{\partial T}{\partial \phi}$$

$$= -A\beta[K_1\{\beta\rho \sin(\psi-\phi)\}\cos(\psi-\phi) + K_1\{\beta\rho\sin(\psi+\phi)\}\cos(\psi+\phi)] \qquad (6)$$

If the point is on the outer surface of the helix $(\psi-\phi)$ reduces to $\sin^{-1} a/\rho$ and $(\psi+\phi)$ to $(2\psi - \sin^{-1} a/\rho)$, where a is the radius of the outer surface of the helix. Substituting these values in Eqn.(6), the azimuthal component of the magnetic field $H\phi_s$ just outside the surface of the helix arm is given by

$$H\phi_s = -A\beta[K_1(\beta a) + K_1\{\beta\rho(\sin 2\psi - \frac{a}{\rho}\cos 2\psi)\}(\cos 2\psi - \frac{a}{\rho}\sin 2\psi)] \quad \ldots \quad (7)$$

Now, for an infinitely long helix of radius a, we have, from Ampere's law,

$$I = \oint H\phi_s \, ds = 2\pi a \,.\, H\phi_s \quad \ldots \quad (8)$$

On substitution, the current flowing axially through the helix arms is given by

$$I = -2\pi a \,.\, A\beta[K_1(\beta a) + K_1\{\beta\rho(\sin 2\psi - \frac{a}{\rho}\cos 2\psi)\}\times (\cos 2\psi - \frac{a}{\rho}\sin 2\psi)] \qquad (9)$$

Now, the E_θ-field is given by the familiar relation,

$$E_\theta = Z_0 \,.\, H\phi \qquad (10)$$

where Z_0 is the characteristic wave imdedance.

Substituting the value of $H\phi$ from Eqn. (6), we get,

$$E_\theta = -Z_0 \,.\, A\beta[K_1\{\beta\rho\sin(\psi-\phi)\}\cos(\psi-\phi) + K_1\{\beta\rho\sin(\psi+\phi)\}\cos(\psi+\phi)] \quad \ldots \quad (11)$$

Hence, the transverse voltage tangential to the meridian plane is, from Eqn.(1),

$$V = \int_{-\psi}^{\psi-\sin^{-1}\frac{a}{\rho}} E_\theta \,.\, \rho d\theta = -Z_0 \,.\, 2A[K_0(\beta a) - K_0(\beta\rho\sin 2\psi)] \quad \ldots \quad (12)$$

The upper limit of integration has been chosen to disregard the region inside the helix cylinder since it contributes little to the external field. From Eqns. (9) and (12), the characteristic impedance of the antenna is given as

$$Z_T = \frac{V}{I} = \frac{Z_0}{\pi a\beta} \cdot \frac{K_0(\beta a) - K_0(\beta\rho\sin 2\psi)}{K_1(\beta a) + K_1\left\{\beta\rho\left(\sin 2\psi - \frac{a}{\rho}\cos 2\psi\right)\right\}\left(\cos 2\psi - \frac{a}{\rho}\sin 2\psi\right)} \qquad (13)$$

It is known that the characteristic wave impedance Z_0 is the same as the intrinsic impedance of free space ($= 120\pi$ ohms) for all transverse electromagnetic waves. Now, the phase velocity of the current wave along the two inclined arms of the antenna is reduced in the ratio β_0/β where $\beta_0 = \omega/c$ and the characteristic impedance of the system is inversely proportional to the phase velocity. It thus follows that the impedance will be increased in the ratio β/β_0. Accordingly Eqn. (13) reduces to

$$Z_T = \frac{120}{a\beta_0} \cdot \frac{K_0(\beta a)-K_0(\beta\rho \sin 2\psi)}{K_1(\beta a)+K_1\left\{\beta\rho\left(\sin 2\psi - \frac{a}{\rho}\cos 2\psi\right)\right\}\left(\cos 2\psi - \frac{a}{\rho}\sin 2\psi\right)} \quad \ldots (14)$$

The impedance of a rhombic antenna is found to vary perceptibly only upto a distance of $\lambda/2$ from the input ends (Schelkunoff, 1952); beyond this distance the variation is very small. The average characteristic impedance of the antenna will thus be given by

$$Z_{av} = \frac{1}{l}\left[\frac{120}{a\beta_0}\cdot\int_0^{\lambda/2}\frac{K_0(\beta a)-K_0(\beta\rho\sin 2\psi)}{K_1(\beta a)+K_1\left\{\beta\rho\left(\sin 2\psi-\frac{a}{\rho}\cos 2\psi\right)\right\}\left(\cos 2\psi-\frac{a}{\rho}\sin 2\psi\right)}\,d\rho\right.$$

$$\left.+\left(l-\frac{\lambda}{2}\right)\cdot\frac{120}{a\beta_0}\cdot\frac{K_0(\beta a)-K_0\left(\beta\frac{\lambda}{2}\sin 2\psi\right)}{K_1(\beta a)+K_1\left\{\beta\frac{\lambda}{2}\left(\sin 2\psi-\frac{a}{\lambda/2}\cdot\cos 2\psi\right)\right\}\left(\cos 2\psi-\frac{a}{\lambda/2}\sin 2\psi\right)}\right] \quad \ldots (15)$$

where l is the axial length of each arm.

The expression for the average characteristic impedance is somewhat involved; however, for practical computation a number of approximations may be made, since the effects of some of the terms in the expression are small compared to others. For example, the quantities $\frac{a}{\rho}\cos 2\psi$ and $\frac{a}{\rho}\sin 2\psi$ have little effect on the variation of Z_{av} with ρ. Hence the denominator of the integrand reduces to $[K_1(\beta a)+K_1(\beta\rho\sin 2\psi)\cos 2\psi]$. The above expression is not integrable by any of the known methods. The integration is therefore performed numerically by the standard trapezoidal rule.

It is interesting to note that the expression on the right-hand side of Eqn. (15) is found to attain a constant value as ρ is increased beyond about 15 cm. This is in conformity with our assumption that the impedance is constant except near the input end. As the average characteristic impedance is approximately equal to the input impedance [assumption (a)], the value of the expression on the right-hand side of Eqn. (15) should also represent the input impedance of the antenna at any frequency.

(ii) *Calculation of radiation pattern* :

In deriving expressions for the directivity of an ordinary rhombic antenna, Foster (1937) assumed that the current flows uniformly without attenuation from the input to the termination. This assumption neglects the effect of radiation and the mutual coupling between the arms. The derivation is thus not rigorous; however, it has been found that the shape of the directivity pattern is not particularly critical with regard to current distribution along the arms of the antenna (Christiansen, 1946).

The analysis of Foster, applicable to the case of a rhombic antenna with linear arms, should also hold good in the case of the antenna under study, except for the fact that the axial phase velocity in the helix arms is different from that in free space. Taking this departure into account, it may be readily seen that the relative directivities of the rhomic antenna under study for horizontal and vertical polarisations are approximately given by (Piggott, 1948; Harper, 1941).

$$D_h = A \cos \xi \left(\frac{\sin (\pi l k_1/\lambda_a)}{\pi l k_1/\lambda_a}\right)\left(\frac{\sin (\pi l k_2/\lambda_a)}{\pi l k_2/\lambda_a}\right) \cos \theta - \sin \xi \cos \Delta)$$

$$\times \sqrt{(1-\rho_h)^2+4\rho_h \cos^2 \left(\frac{\alpha_h}{2} - \frac{2\pi H}{\lambda} \sin \Delta\right)} \tag{16}$$

and

$$D_v = A \cos \xi \left(\frac{\sin (\pi l k_1/\lambda_a)}{\pi l k_1/\lambda_a}\right)\left(\frac{\sin (\pi l k_2/\lambda_a)}{\pi l k_2/\lambda_a}\right) \sin \theta \,.\, \cos \Delta$$

$$\times \sqrt{(1-\rho_v)^2+4\rho_v \cos^2 \left(\frac{\alpha v}{2} - \frac{2\pi H}{\lambda} \sin \Delta\right)} \tag{17}$$

where (figure 6),

l is the axial length of each arm ;

ρ_h, ρ_v —reflection coefficients of the ground, the suffixes h and v referring to the horizontal and vertical components;

α_h, α_v —phase changes due to the reflection;

Δ—elevation angle of the main radiation lobe with reference to the plane of the antenna;

2ξ —obtuse angle subtended by the adjacent helix-arms;

θ—aximuth angle of the axis of the major lobe referred to the major axis of the antenna;

H—height above the ground;

λ—free-space wavelength at the given frequency;

λ_a—effective 'axial' wavelength corresponding to frequency 'f' given by $\lambda_a = \frac{v}{f}$ where $v = \sin\alpha$;

$$k_1 = \frac{c}{v} - \cos\Delta \,.\, \sin(\xi+\theta)$$

$$k_2 = \frac{c}{v} - \cos\Delta \,.\, \sin(\xi-\theta)$$

k_1 and k_2 refer to the pick-up in the two pairs of the rhombic arms.

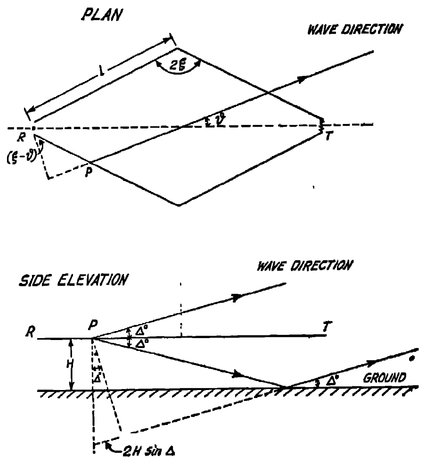

Fig. 6.—Illustrating the plan and the side elevation of the antenna when erected horizontally above the "ground".

For a perfectly conducting ground $\rho_h = 1$ and $\alpha_h = \pi$. The ground reflection factor in Eqn.(16) in case of the horizontally polarised component thus reduces to

$$R_h = 2\sin\left(\frac{2\pi H}{\lambda}\sin\Delta\right) \qquad \ldots \quad (18)$$

For the vertically polarised component, however, both ρ_v and α_v are dependent on Δ and so, the reflection function, in Eqn.(18) hereafter represented by R_v, cannot be so replaced by a simple expression as in the case of R_h. Nevertheless, for approximate calculations, we may take $R_v \doteq 1$ for $\Delta \doteq 17.5°$ (Hamer, 1953).

It is seen from Eqns. (16) and (17) that the polar diagrams of the rhombic aerial are controlled by the product of three factors, viz., the integral functions $\frac{\sin(\pi l k_1/\lambda_a)}{\pi l k_1/\lambda_a}$, $\frac{\sin(\pi l k_2/\lambda_a)}{\pi l k_2/\lambda_a}$; the ground-reflection functions R_h, R_v ; and the projection functions $(\cos\theta - \sin\xi \cos\Delta)\cos\xi, (\sin\theta \, . \cos\Delta)\cos\xi$. It is apparent that if any of these factors is zero, the directivity must also be zero. This determines the positions of minima in the radiation pattern.

The ground-reflection functions (R_h, R_v) are dependent on Δ and H/λ and so, are fixed by the design of the antenna. For a particular frequency, the positions of maxima and minima in the polar diagram are dependent on the values of the projection functions as well as the integral functions. The shape of the polar diagram, however, is predominantly controlled by the integral function, or in other words, by the values of l/λ_a and k_1, k_2.

It is necessary that all the three functions should be large if a large directivity is required. In the case of the antenna under study, the values of the ground-reflection function and the projection function remain the same as in the case of a rhombic antenna with linear arms, but k_1 and k_2 assume very large values. These increments in the values of k_1, k_2 are due to the reduction in the phase velocity v. The magnitudes of the integral function thus are reduced, thereby causing a reduction in the value of the directivity of the antenna under study.

The directivity patterns, particularly for the horizontal polarisation in the azimuthal plane, show reasonable agreement with the theoretical values. The vertically polarised components of the field are present, though in smaller amplitudes, almost in the same direction as the horizontal components. This shows that the radiation field is somewhat elliptically polarised. The directivity patterns of the vertical components do not agree well with the theoretical values. This is

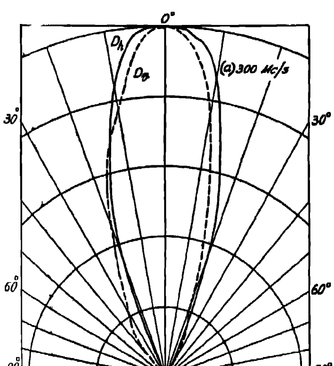

Fig. 7 (a).

D_h and D_v patterns of the antenna at 300 Mc/s.

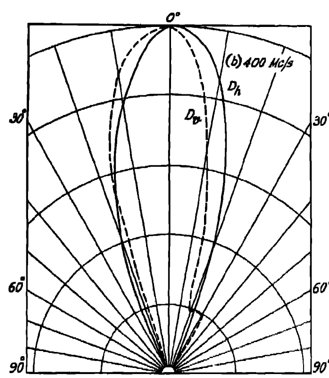

Fig. 7 (b).

D_h and D_v patterns of the antenna at 400 Mc/s.

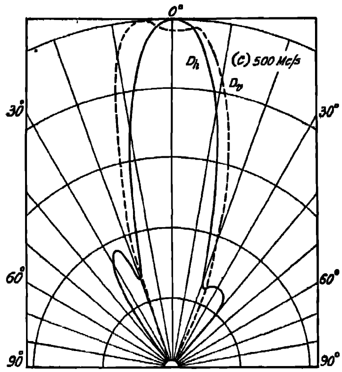

Fig. 7 (c).

D_h and D_v patterns of the antenna at 500 Mc/s.

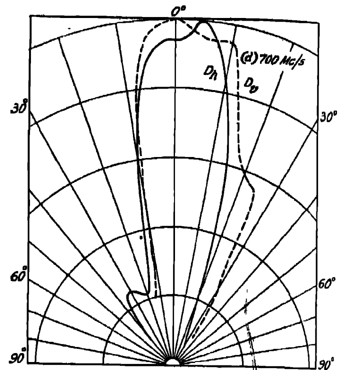

Fig. 7 (d).

D_h and D_v patterns of the antenna at 700 Mc/s.

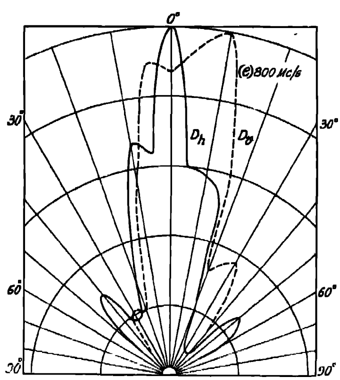

Fig. 7 (e).

D_h and D_v patterns of the antenna at 800 Mc/s.

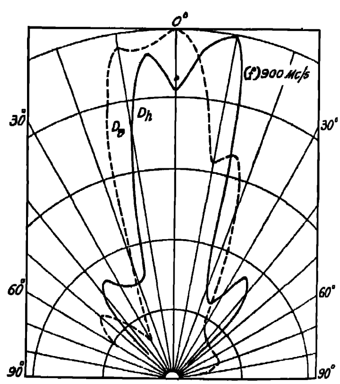

Fig. 7 (f).

D_h and D_v patterns of the antenna at 900 Mc/s.

as one would expect, for the derivation of the expressions for the directivity has been based on the assumption that the current in each helix arm can be replaced by an axial current which is not strictly true.

The patterns (figures 7-9) have been plotted after normalising the values. In figure 8, the experimental and theoretical polar diagrams of the antenna under study are compared for 600 mc/s excitation. Figure 9 has been shown to compare the theoretical polar plots (D_h) for the antenna with cylindrical helices as the arms and that with linear arms also at 600 mc/s excitation.

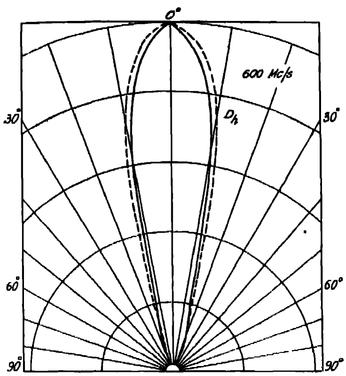

Fig. 8.

Calculated (dotted lien) and observed (solid line) D_h patterns at 600 Mc/s.

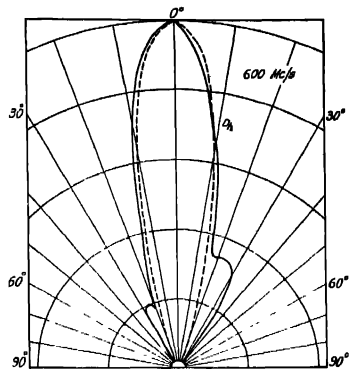

Fig. 9.

Calculated D_h patterns of the rhombic antenna with linear arms (dotted line) and of that with cylindrical helices as the arms (solid lines). Frequency, 600 Mc/s.

4. CONCLUDING REMARKS

It is evident from the observed impedance and the radiation characteristics of the antenna with helix arms that the wide-band properties and the directivity characteristics of a rhombic antenna with linear arms are more or less maintained in the case under study. There is, however, a decrease in gain. The reason may possibly be ascribed to the lesser "effective area" of the antenna under study in contrast to a corresponding antenna with linear arms.

It is found that at a particular frequency, the average characteristic impedance varies inversely as the radius of the helix cylinders. The impedance, again, varies from point to point near the input end and becomes constant after a distance. If the helices are suitably tapered towards the input ends the variation of impedance in the region may be reduced thereby enabling better match with the feeders.

ACKNOWLEDGMENTS

The author is grateful to Professor S. K. Mitra, F.R.S., for his kind interest in the work and to Professor J. N. Bhar for constant encouragement and enlightening discussions during the preparation of the paper. It is a pleasure to record his appreciation of the help and suggestions obtained from Professor J. S. Chatterjee and Mr. N. B. Chakravorty in course of the work. Thanks are also due to Mr. A. K. Choudhury for assistance in connection with the measuring equipments.

REFERENCES

Christiansen, W. N., 1947, *A.W.A. Technical Journal*, **7**, No. **4**, 372.

Hamer, E. G., 1953, *Electronic Engg.*, **25**, 427.

Harper, E., 1941, Rhombic Antenna Design, D. Van Nostrand, New York,

Foster, D., 1937, *Proc. I.R.E.*, **25**, 1327.

Kraus, J. D., 1954, Antennas, McGraw-Hill Book Company, Inc., New York.

Neimann, M. S., 1939, *Izvestiya Electroprom, Slab. Joka*, No. 1, **19**.

Piggott, W. R., A method of determining the Polar Diagrams of Long Wire and Horizontal Rhombic Aerials", 1948, D.S.I.R (U.K.), Radio Research Special Report, No. 16.

Pocklington, H. C., 1897, *Proc. Caml Phil. Soc.*, **9**, 324.

Schelkunoff, I. S., 1943, Electromagnetic Waves, D. Van Nostrand, New York, 441.

Schelkunoff, I. S. and Friis, H. T., 1952, Antennas: Theory and Practice, John Wiley and Sons, New York, 427, 107.

Smith, W., Antenna Manual, Editors and Engineers Ltd., California, U.S.A., 213.

Tomiyasu, K., 1949, *J.A.P.*, **20**.